5-AXIS DRY MILLING OF BOTTOM OF POCKET BY BALL AND CIRCLE-SEGMENT END MILLS

ALES POLZER, VIT SEBESTA, TOMAS TRCKA

Brno University of Technology, Faculty of Mechanical Engineering, Institute of Manufacturing Technology,

Brno, Czech republic

DOI: 10.17973/MMSJ.2020_03_2019153

e-mail: polzer@fme.vutbr.cz

At present, 5-axis machining is often realized with ball end mills that do not achieve the advantages of modern circle - segment end mills. However, to exploit the potential of these modern tools, it is necessary to use a special CAM software, including hyperMILL from Westcam. This software, increasing the efficiency of machining, was used in the present study, which compared these tools with respect to the quality of the machined surface, machining time and cutting forces. The workpiece material was aluminum alloy EN AW 7075-T6. At given cutting parameters, the circle-segment end mills achieved a lower **Ra** value and generally higher machining efficiency. At the end of the study, an assessment was made with respect to the economy.

KEYWORDS

hyperMILL, CNC programming, machined surface, force measurement, circle-segment end mill.

1 INTRODUCTION

Nowadays CAM programs are almost indispensable, if safe and effective manufacturing is demanded. In addition to capability of simple modeling, they especially can give confirmation after paths programming, if there are no collisions between the machine, clamp or workpiece.

The tool axis is fixed in conventional 3D machining. Spatial milling interpolation is done only through three linear motions, which greatly simplifies the way NC data is programmed. However, in case of end ball mills when finishing, unfavorable engagement conditions together with zero cutting speed in the tool axis have a detrimental effect on the entire cutting process. This caused the chip *forging*, increasing the cutting temperature and creating a build-up edge, resulting in a poorly machined surface and reduction of the tool life (chipping of the cutting edge may occur).

This negative effect can be eliminated by multi-axis milling (Fig. 1), the so-called tilting of the tool in the fourth direction, respectively fifth axis. This caused an increase of effective diameter ($\mathbf{d_{eff}}$) at the same value of $\mathbf{a_p}$. Optimal tilting of the tool in terms of cutting-edge wear, process reliability, accuracy and roughness of the machined surface was found to be 10° to 20° in the feed direction ($\boldsymbol{\beta_f}$) while climb milling [Sadilek 2013] [Skopecek 2005]. A new innovative strategy of the software hyperMILL developed by the OPENMIND company support this just as an issue of plane tangential milling using barrel mills.

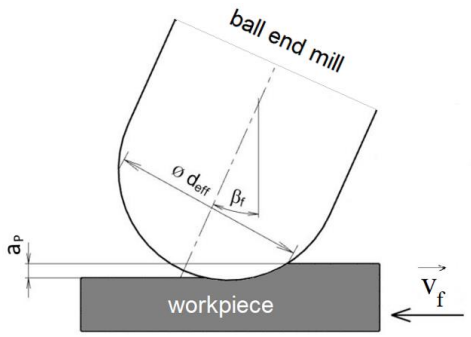

Figure 1. Tilting of the Tool - Pulled Method [Sadilek 2013]

This study deals with 5-axis machining of the planar bottom of the pocket using mentioned software and special tools, which was supported by experimental measurements to obtain real data for evaluation. This possibility of innovative milling is not very widespread in practice despite its higher efficiency, mainly due to the necessity of acquiring a 5-axis milling machine and advanced software.

2 EXPERIMENTAL SET UP

An experiment was performed at the Technology Institute of the Mechanical Engineering in Brno on a 5-axis milling machine MCV 1210 Tajmac ZPS equipped with an OMP400 probe.

The workpiece material used for the experiment was aluminum alloy EN AW 7075 – T6. It has reduced corrosion resistance (in comparison to EN-AW 6082 alloy, caused by copper), is well machinable and polishable and dominates by its high strength against other aluminum alloys [*Ehlinik* 2019]. Material was delivered heat treated (T6). Chemical composition and physical properties are stated in Tab. 1 and Tab. 2.

%Si	%Fe	%Cu		%Mn	%Mg		%Cr		%Zn		%Ti	%Al
max	max	min	max	max	min	max	min	max	min	max	max	-
0.4	0.5	1.2	2	0.3	2.1	2.9	0.18	0.28	5.1	6.1	0.2	BALANCE

Table 1. Chemical Composition of Aluminum Alloy EN AW 7075 [*Alunet* 2019]

$R_{p0,2}$ [MPa]	R_m [MPa]	A [%]	HBS	Density [g/cm³]	E [GPa]
440	525	4	155	2.81	72
Thermal expansion coef. [cm*K]	**Thermal conductivity [W/K*cm]**	**Melting temperature [°C]**	**Electric conductivity [Ω *mm²]**		**Weldablitiy**
23.3	1.3-1.6	500-640	17-20		LOW

Table 2. Physical Properties of Aluminum Alloy EN AW 7075 [*Alunet* 2019]

Tested tools 2550A.008 and 3540.1615AA by the company EMUGE-FRANKEN were used – see Fig. 2. A circle-segment end mill was clamped into a hydraulic holder marked as HSK 63A HC2090 by Pramet and a ball end mill was clamped into GM 300 from Gühring. Since high-speed cutting (HSC) was used, it was needed to use small tool overhang to minimize vibrations that could lead to a tool failure [Toh 2004]. Due to diameters (rigidity) of tools and dynamics of the machining process, this value was 55 mm for the circle segment end mill and 30 mm for the ball end mill. In high-speed milling, cooling by the cutting fluid is not generally required, so the process went without cooling as dry machining [Rasa 2002], which is an environmentally friendly direction.

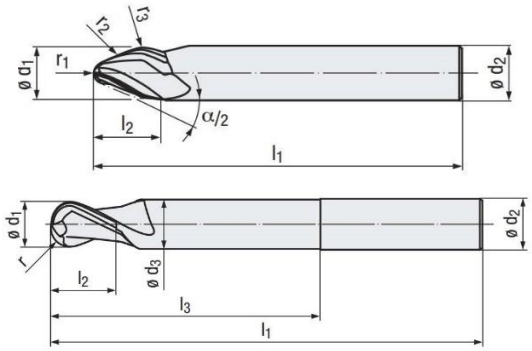

Figure 2. Experiment Tools [EMUGE-FRANKEN 2016] [EMUGE-FRANKEN 2017]

In Table 3, the necessary cutting conditions can be found for carrying out the experiment, where step a_p is a step in the **Z** axis (height step indicated in Fig. 3) and a_e indicates the material removal depth. Diameter d_1 was the nominal value of the tool cutting diameter and shank. Dimension **r1** for the circle-segment end mill was identical to dimension **r** for the ball end mill - 4 mm, see Fig. 2. The cutting speed was limited by the machine, on which the experiment was performed, thereby revolutions

	Qua-ntity	Unit	Ball end mill	Circle-segment end mill
Revolutions of the spindle	n	[min^{-1}]	14 000	10 000
Cutting speed	v_c	*[m· min^{-1}]*	*352*	*503*
Feed per tooth	f_z	[mm]	0.03	0.03
Radial depth of the cut	a_e	[mm]	0.5	0.5
Axial depth of the cut	a_p	[mm]	0.320	6.197
Tool diameter	⌀d_1	[mm]	8	16
Cutting fluid		Dry		
Air cooling with atmospheric pressure				
Climb milling				

Table 3. Selected Cutting Conditions

14 000 min^{-1} (v_c = 352 m·min^{-1}) was chosen for the ball end mill. Revolutions of 10 000 min^{-1} was calculated for the circle-segment end mill, due to different in effective diameter (d_{eff}). The cutting speed was at the maximum cutting diameter 503 m·min^{-1} and in direction towards tool axis decreased to 100 m·min^{-1} (**r1** = 4 mm). Values of a_p were chosen from the calculation ensuring the same theoretical roughness of the machined surface by both tools.

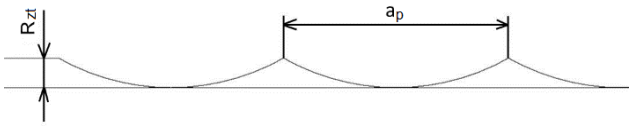

Figure 3. Surface Irregularities when Milling

This calculation of the theoretical roughness was based on the assumption that the machined workpiece is absolutely non-deformed, the tool edge produces geometrical curves and that the machine-tool-workpiece assembly is rigid [Potacel 2004] [Sandvik 2019]. The theoretical calculation of the maximal profile height **Rzt** can be done by the equation (1). The theoretical calculation of the roughness **Ra** for spherical cutters can be done by the equation (2) [Davim 2010] [Potacel 2004]:

$$Rzt = r_\varepsilon \cdot \left(1 - \sqrt{1 - \left(\frac{a_p^2}{4 \cdot r_\varepsilon^2}\right)}\right)[mm] \quad (1)$$

$$Ra = \frac{10^3 \cdot r_\varepsilon^2 \cdot (2 \cdot \alpha_A - \sin(2 \cdot \alpha_A))}{a_p}[mm] \quad (2)$$

where α_A can be calculated as:

$$\alpha_A = \arccos\left[\frac{r_\varepsilon}{a_p} \cdot \left(\arcsin\left(\frac{a_p}{2 \cdot r_\varepsilon} + \frac{a_p}{4 \cdot r_\varepsilon^2} \cdot \sqrt{4 \cdot r_\varepsilon^2 - a_p^2}\right)\right)\right][mm] \quad (3)$$

Tab. 4 shows the results of the theoretical calculation of **Rzt** and **Ra**. These results were verified by a geometrical method (Fig. 3). The mean height of the roughness of the profile **Ra** subtracts all deviations from the middle line of the profile on the evaluated length, regardless of their vertical direction. From this it can be concluded that the **Ra** value cannot be used to determine whether the elevation deviations have the character

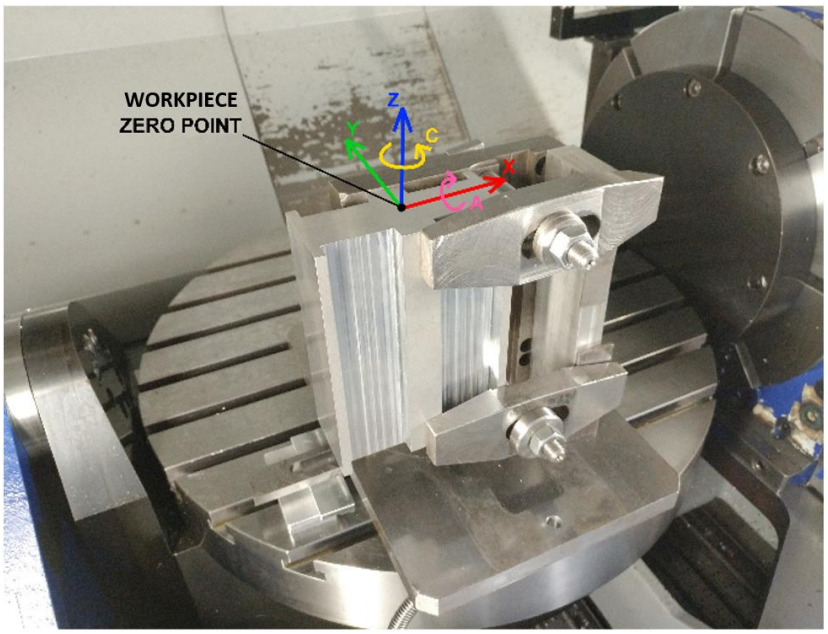

Figure 4. Clamped Workpiece by Angle Fixture and Machine Coordinate System

of protrusions or depressions (groove). The **Ra** value is not significantly influenced by sporadic deviations, which means there is a risk of neglecting a large protrusion or groove [Forejt 2006].

	Ra [µm]	**Rzt** [µm]
Ball end mill	0.821	3.201
Circle-segment end mill	0.821	3.201

Table 4. Calculated Theoretical Surface Roughness Values

Fig. 4 shows the coordinate system on a given workpiece with a roughed pocket. An experimental milling was carried out at the bottom of the pocket – see Fig. 5 and 6. The width of one groove was 40 mm. During the programming, a problem in the tool path simulation occurred as a collision between the tool clamp and the workpiece when using a ball mill. This problem with the ball end mill was eliminated with the use of the hyperMILL tool tilt program function in imminent collision. This determined the maximum tilt angle of the tool, which was set as primary to keep the process constant (remaining at 35.242°). The circle-segment end mill was tilted by 20° - see Fig. 2 and parameter **α/2**.

3 RESULTS AND DISCUSSION

To verify the roughness of the workpiece surface, a roughness measurement device TR100 was used. The roughness was measured in the transverse direction of the milled pocket (in the **Z** direction) so that the diamond tip of the measuring instrument could evaluate the surface irregularities as shown in Fig. 3. The measurement confirmed the theoretically calculated values. - see Tab. 5. It can also be deduced, when using a circle - segment end mill, not only a higher value of $\mathbf{a_p}$ was achieved, but also an increase in the surface quality compared to a ball end mill at given cutting parameters.

	Ra [µm]	**Rzt** [µm]
Ball end mill	0.85 ± 0,06	4.1 ± 0,21
Circle-segment end mill	0.56 ± 0,25	2.26 ± 0,57

Table 5. Measured Surface Roughness Values

The measuring of cutting forces was performed by dynamometer Kistler 9257B. The dynamometer sampling rate for this experiment was set to 6 kHz, which means 36 recorded values during 1 revolution for a ball end mill and 25,7 values for a circle-segment mill.

Figures 5 and 6 show a position of the tool during machining. When seeing these two sets of Figures, it can be assumed that the orientation of some force vectors will change with respect to a symmetrical machining. In the position 2, the table of the machine was reversed from pulling the workpiece out to pushing the workpiece into the table.

Figures 7 and 8 show the trend of forces after the dynamometer measurement as the machining proceeded. The total cutting force **F** is the force resultant of all 3 individual forces and is calculated from a relation (4). Since a stationary dynamometer was used, a second measurement of the machine dynamics itself had to be made and these two processes were subtracted from each other to obtain the independent real milling force (Fig. 9 and Fig. 10). Comparing Fig. 7 and 9 (respectively Fig. 8 and 10), the dynamics forces of the machine greatly exceed the force values of the milling cutter. For the ball end mill, the difference between these values was 158 N, and for the circle-segment end mill up to 405 N. High fluctuations in the force values at the beginning of the cutting process were caused by a rapid approach to the cut. Rotating multi-component dynamometer would have been better to measure acting forces because of the more accurate force record.

$$F = \sqrt{F_x^2 + F_y^2 + F_z^2} \tag{4}$$

When analysing the 5-axis milling with a complex movement of the tool after the subtraction of table dynamics in Fig. 9 and 10, the force $\mathbf{F_x}$ was very low and the most significant force impact was by the forces $\mathbf{F_y}$ and $\mathbf{F_z}$. Figures 5 and 6 graphically illustrate the forces of the acting tools. When comparing the force output of the ball end and circle-segment end mill, trends of forces were the same, but their size was different in proportion of the cross section of the chip being removed, which

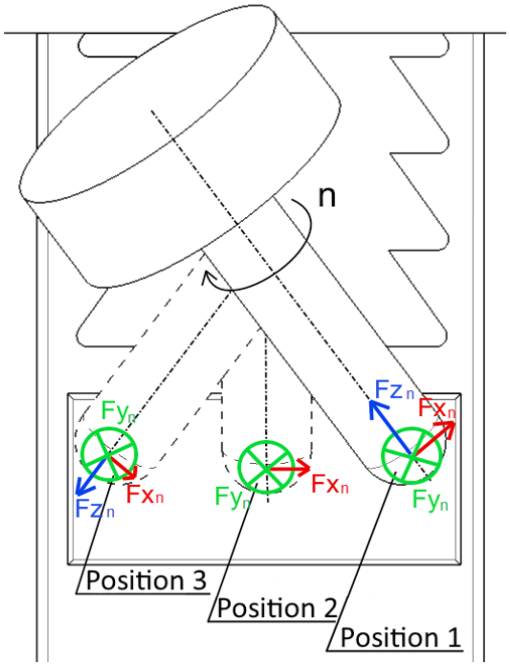

Figure 5. Schematic of the Cutting Process with Ball End Mill

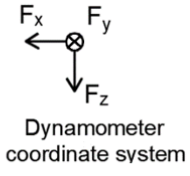

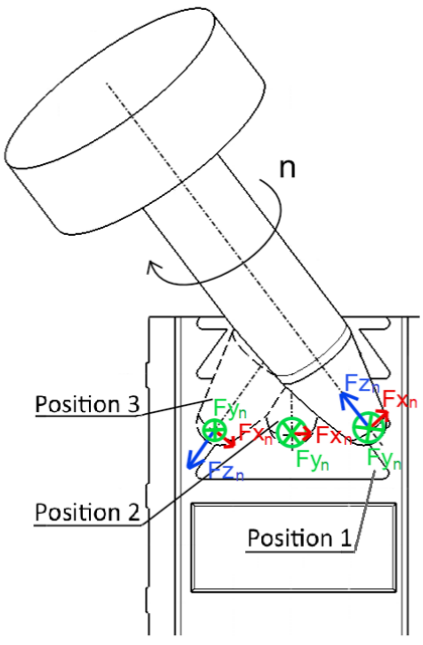

Figure 6. Schematic of the Cutting Process with Circle-Segment End Mill

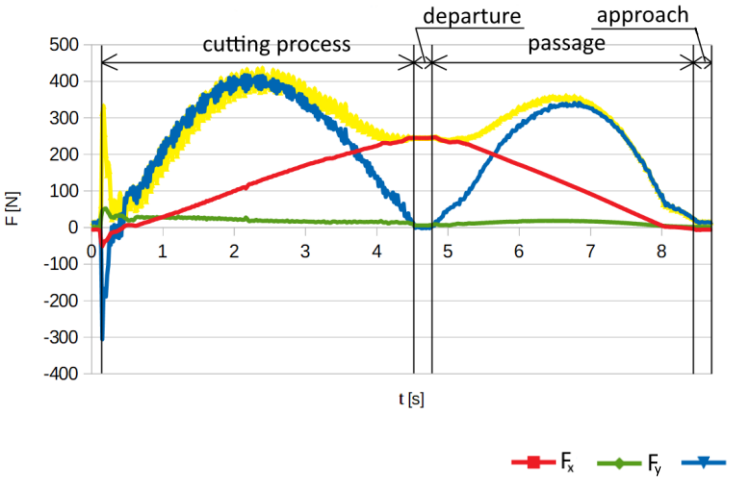

Figure 7. Force Output of the Circle-Segment End Mill with Table Dynamics

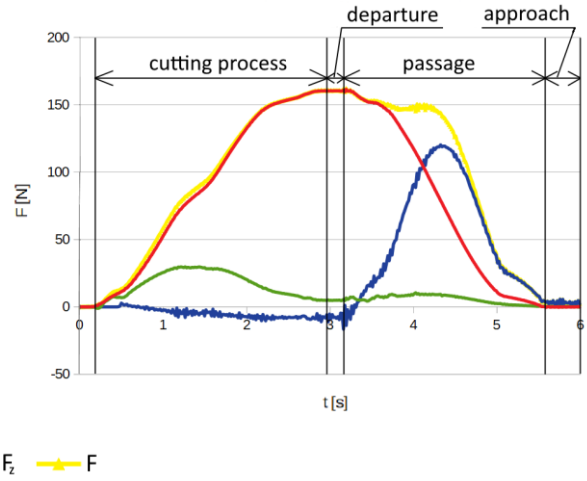

Figure 8. Force Output of the Ball End Mill with Table Dynamics

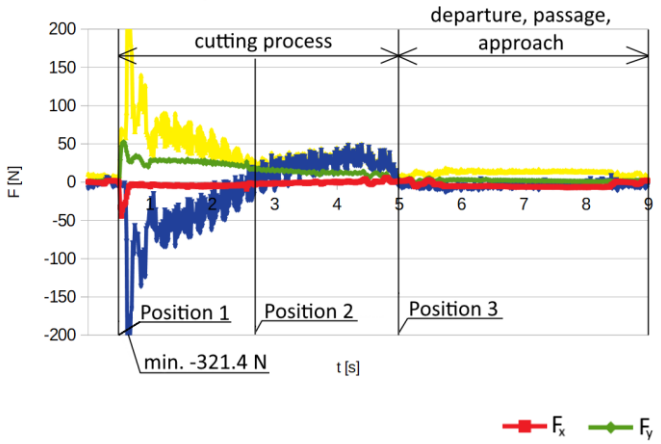

Figure 9. Force Output of the Circle-Segment End Cutter After Subtraction of Table Dynamics

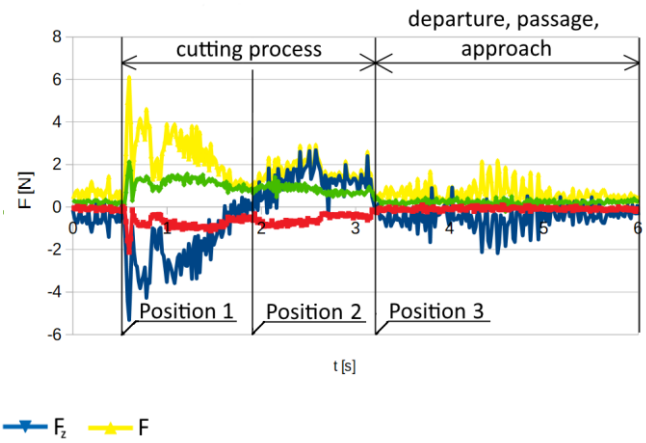

Figure 10. Force Output of the Ball End Cutter After Subtraction of Table Dynamics

is associated with the application possibilities of both tools. The circle-segment end mill is not appropriate to use on thin-walled components. The possible wall deflection and increased vibration could occur in that case. Minor fluctuations in force $\mathbf{F_z}$ (position 2 in Figure 9 and 10) occurred because of a table reversal. The total cutting force **F** is highest at position 1 for both tools, as the chip of the largest cross-section was machined when approaching the cut.

Fig. 11 shows the final workpiece after machining. Using a circle-segment end mill it is possible to notice the inaccurate approach of the mill to the cutting point, which is recognized by the small milled surfaces on the side wall of the pocket. This incident was caused by inaccurate clamping. This mark was not found on the other side of the pocket.

The economic analysis in Fig. 12 was specified by milling the entire pocket using a circle-segment end mill and ball end mill with a tool life of 300 minutes. This Figure shows that from the

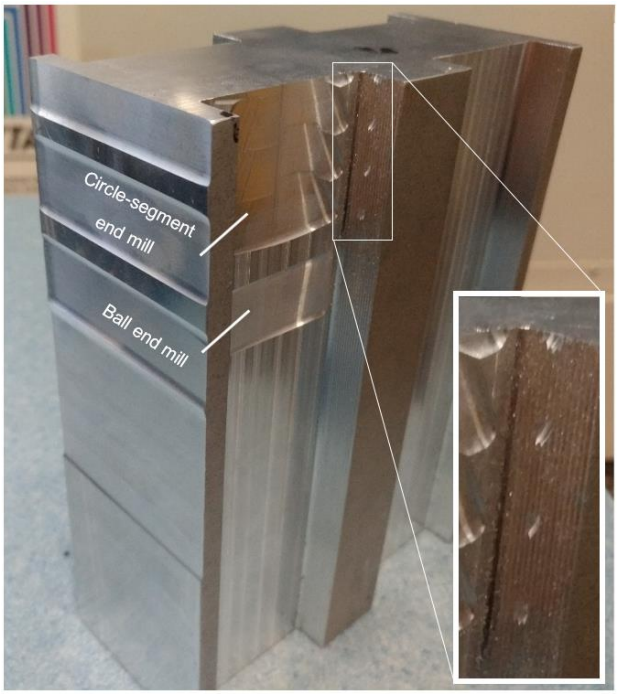

Figure 11. Final Piece

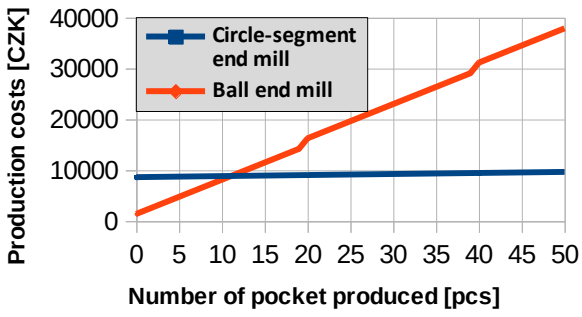

Figure 12. Economical Comparison of Circle-Segment and Ball end mills

12th manufactured pocket, it is cheaper to use the circle-segment end mill instead of the ball end cutter. This is due to the initial increased cost of this cutter. The difference of the value of a_p is 19 times bigger at the circle-segment end mill instead of ball end cutter, thus by using the circle-segment end mill, the time of machining will be 19 times smaller. The machine times were obtained by the program hyperMILL. Under the given conditions and tool life, the ball end tool needs to be replaced after 20 manufactured pockets, while the circle-segment end mill after 153 produced pockets.

This article came to same conclusions as [Urbikain 2019] in terms of static forces of 3+2D milling and also to the same conclusions as the work [Urbikain 2018] in terms of measured roughness. Deviations may have been caused by different cutting conditions.

4 CONCLUSION

Comparisons of advantages of modern circle - segment end mill and ball end mill were performed using the special CAM software – hyperMILL – for programming when dry - environmentally friendly - machining. This software was chosen as more suitable for this experiment.

The experimental measurement of roughness values confirmed theoretically calculated values. When the calculated maximum profile **Rzt** for both mills were 3,2 µm, the value of a_p for the ball end mill was more than 19 times smaller than for the circle-segment end mill with these geometrical parameters of tools. This implies that the machined surface contains fewer transitions between the individual toolpaths. Measured values of **Rzt** and **Ra**, which were smaller for circle-segment end mills, confirmed that.

At given cutting parameters, using the circle-segment end cutter would bring 19 times the time savings as opposed to a ball end cutter. The turning point of production economy has a value of 12 produced pockets from where it is cheaper to use the circle-segment end mill. This is due to the initial increased cost of this cutter. The difference in the product price increases with the number of pieces produced by the milling cutters. However, higher productivity is also redeemed by a significantly higher load on the circle-segment cutter.

In the manufacturing process, the cutting conditions must be optimized. The effect of high forces of the circle-segment end mill was caused by the cross section of the chip being removed. Thorough clamping of workpieces, deflection of thin walls and vibrations of machined parts, which could lead to chipping, could occur, which should also be taken into account. Another drawback may be the more complicated programming and universality of use. In all other parameters, the circle-segment end mill showed clear advantages over the ball end mill. The use of a circle-segment end cutter is more advantageous in finishing operations.

CONTACT:

Ing. Ales Polzer, Ph.D.
Brno University of Technology,
Faculty of Mechanical Engineering,
Institute of Manufacturing Technology,
Technicka 2896/2, 616 69 Brno, Czech Republic
e-mail: polzer@fme.vutbr.cz

ACKNOWLEDGMENTS

This article was supported by the FME BUT Brno, Czech Republic as a specific research FSI-S-19-6014 called "Research of perspective manufacturing technologies".

REFERENCES

[Alunet 2019] *Alunet*. Custom made aluminium profiles (in Czech). *ALUCAD Bohemia*, 2019, Pardubice, [online]. 2019 [cit. 2019-09-15]. Available from: http://www.alunet.cz/technicke-udaje

[Davim 2010] Davim, J. P. Surface Integrity in Machining. London: *Springer*, 2010. ISBN 978-1-84882-873-5

[Ehlinik 2019] *Ehlinik*. Aluminum alloys (in Czech). *A + A Pardubice spol*, 2019, Pardubice, [online]. 2019 [cit. 2019-08-17]. Available from: https://www.ehlinik.cz/prilohy/zakladni-technicke-informace.pdf

[EMUGE FRANKEN 2016] EMUGE FRANKEN. Universal End Mills for the Die and Mould Industry. Germany: *EMUGE-FRANKEN*, 2016

[EMUGE FRANKEN 2017] EMUGE FRANKEN. Circle Segment End Mills. Germany: *EMUGE-FRANKEN*, 2017

[Forejt 2006] Forejt, M. and Piska, M. Theory of machining, forming and tools (in Czech). Brno: *Academic Publishing house CERM*, 2006. ISBN 80-2114-2374-9

[Potacel 2004] Potacel, V. Technological standpoints of surface texture while finish machining (in Czech). Ph.D. Thesis, Brno: *Institute of Manufacturing Technology*, 2004. ISBN 8021426918

[Rasa 2002] Rasa, J. and Kerecaninova, Z. Important aspects of high-speed milling (in Czech). *MM Prumyslove spektrum*, December 2002, Vol. 12, pp 16. ISSN 1212-2572. Standart number: 021284

[Sadilek 2013] Sadilek, M. Evaluation of machined surface condition after multi-axis milling (in Czech). Project *Integrita*, 2013, Plzen [online]. 2013 [cit. 2019-04-02]. Available from https://www.integrita.zcu.cz/download/skola2/ostrava_prez1.pdf

[Sandvik 2019] Sandvik Coromant. Measurement of workpiece surface quality (in Czech). Sandvik Coromant, 2019, Sandviken [online]. 2019 [cit. 2019-04-08]. Available from: https://www.sandvik.coromant.com/cs-cz/knowledge/materials/pages/workpiece-surface-measurement.aspx

[Skopecek 2005] Skopecek, T. and Hofmann, P. Milling strategies in mold and die production: Machining (in Czech). *MM Prumyslove spektrum*, May 2005, Vol. 5, pp 22. ISSN 1212-2572. Standart number: 050509

[Toh 2004] C.K. Toh. Vibration analysis in high speed rough and finish milling hardened steel. *Elsevier*, November 2004, Vol. 278, No. 14, pp 101-115. ISSN 0022-460X

[Urbikain 2018] G. Urbikain, L. N. Lopéz de Lacalle. Modelling of surface roughness in inclined milling operations with circle-segment end mills. *Elsevier*, May 2018, Vol. 84, No. 15, pp 161-176. ISSN 1569-190X

[Urbikain 2019] Gorka Urbikain, P. Modelling of static and dynamic milling forces in inclined operations with circle-segment end mills. *Elsevier*, March 2019, Vol. 56, No. 12, pp 123-135. ISSN 0141-6359